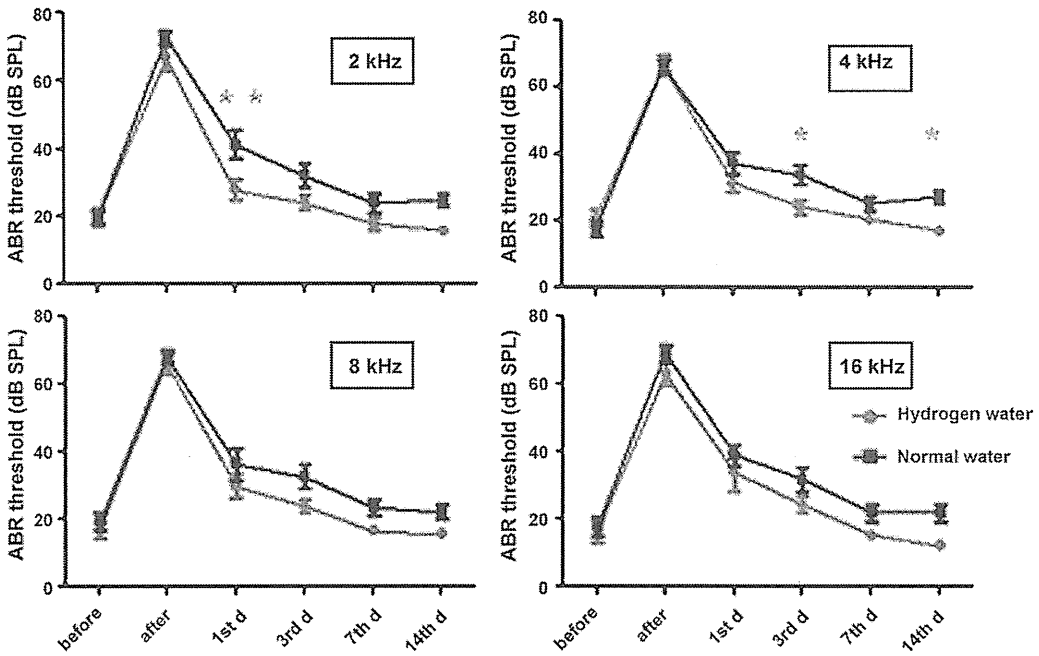

Fig. 2. Thresholds of auditory brainstem response (mean ± S.D.) measured before, immediately after noise exposure and post-noise 1st day, 3rd days, 7th days, 14th days in normal water-treated controls and hydrogen-treated animals ($n = 12$ in each group). There is a statistical significance at all frequencies (two-way ANOVA) and post-noise 1st day for 2 kHz, 3rd day and 14th day for 4 kHz with Bonferroni post-tests (**$p < 0.01$, *$p < 0.05$).

The overall effect of hydrogen significantly attenuated the TTS across the measurement period for all the tested frequencies ($p < 0.05$). Compared to the controls, the hydrogen-treated animals showed significantly smaller ABR thresholds at 2 kHz on day 1 day after noise exposure ($p < 0.01$) and at 4 kHz on day 3 and 14 after noise exposure ($p < 0.05$).

Fig. 3 shows the mean DPOAE input/output (I/O) growth functions at 16 kHz before and immediately, 1, 3, 7, and 14 days after noise exposure. There was no statistically significant difference between the 2 groups considering the amplitude of DPOAE I/O function. Both the groups showed a severe decrease in DPOAE amplitude immediately after noise exposure. Compared to the controls, the hydrogen-treated animals showed greater amplitudes during the recovery process. The overall effect of hydrogen water application was statistically significant 3 and 7 days after noise exposure ($p < 0.01$), although both groups exhibited almost normal I/O function 14 days after noise exposure.

The present study showed that hydrogen attenuated noise-induced TTS and accelerated the recovery of DPOAE. It is likely that hydrogen facilitates the recovery of hearing function because of its antioxidant property [1]. A previous *in vitro* study has also demonstrated the potential of hydrogen to protect both the inner hair cells and outer hair cells from oxidant damage induced by different concentrations of antimycin A [16]. Incubation with a hydrogen-saturated medium significantly reduced ROS generation and subsequent lipid peroxidation in the auditory epithelia, leading to increased survival of hair cells. Hydrogen selectively alleviates hydroxyl radicals (•OH) and peroxynitrite radical ($ONOO^-$)-induced cytotoxicity without affecting other ROS, such as superoxide ($O_2^{\bullet -}$), hydrogen peroxide (H_2O_2), or nitric oxide ($NO^\bullet$) [23]. Thus, it is unlikely that hydrogen disturbs metabolic oxidation–reduction reactions or disrupts ROS involved in cell signaling. This characteristic of hydrogen is advantageous in medical treatments because the use of hydrogen should not cause serious unwanted side effects.

In the current study, we did not examine the morphological changes in the cochlea because the abnormalities in ABR and DPOAE measurements were minimal 14 days after noise exposure. The physiological findings, however, suggest that the noise level used in the current study induced only subtle morphological changes such as bleb formation, but not severe degeneration such as apoptosis of the outer hair cells. No significant permanent morphological changes have been shown in the hair cells in previous studies using a similar protocol of noise exposure [22]. In contrast, it has been shown that in guinea pigs, the afferent dendrites beneath the inner hair cells become swollen immediately after exposure to similar noise causing TTS [28]. Kujawa and Liberman [17] have reported that acoustic overexposures causing moderate, but completely reversible threshold elevation leave cochlear sensory cells intact but cause acute loss of the afferent nerve terminals and delayed degeneration of the cochlear nerve in mice. Although the difference of ABR thresholds immediately after noise was small between hydrogen-treated animals and controls, therefore, it is considered intriguing to examine if hydrogen attenuates such acute and chronic changes of the neural elements.

The efficacy of any single antioxidant may be limited by several factors, including limited access to cellular compartments, action against only a few forms of ROS, interference with redox-based signaling, or a tendency to throw innate ROS protections out of balance [22]. Thus, despite its mild effect, molecular hydrogen is still an optimal choice. It reacts only with the strongest oxidants. Besides, it can penetrate biological membranes by gaseous rapid diffusion and target organelles like the mitochondria and nucleus, which makes it highly effective for reducing cytotoxic radicals. This unique feature of molecular hydrogen is especially favorable for drug delivery to the inner ear compared to other antioxidants, because the blood–labyrinthine barrier blocks many therapeutic compounds and does not allow them to reach cochlear hair cells.

The present study shows that hydrogen can promote hearing recovery from acoustic trauma-induced TTS and can attenuate TTS. This improvement likely reflects hydrogen's scavenging of detrimental ROS. Since hydrogen has already been used in humans clinically to treat decompression sickness in divers with few or no side effects, our findings reinforce the potential clinical utility of

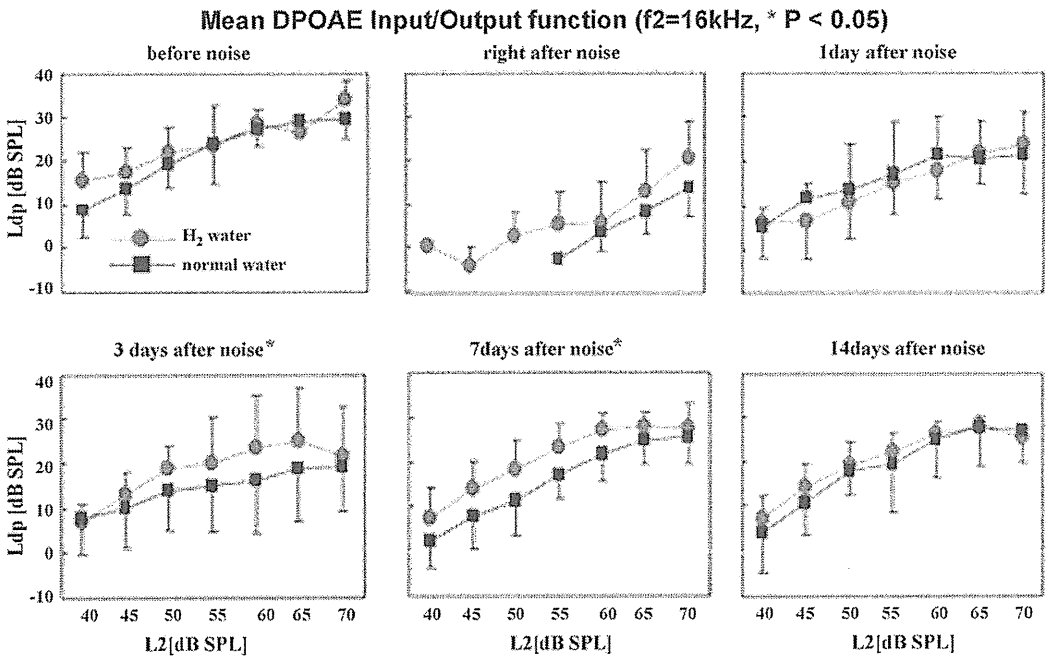

Fig. 3. Mean DPOAE input–output function at different time points at f2 = 16 kHz in normal water-treated controls and hydrogen-rich water-treated animals ($n = 5$ in each group). There is a statistical significance on post-noise days 3 and 7 days. $^*p < 0.05$.

hydrogen as an adjuvant agent for noise-induced hearing loss in humans.

Acknowledgments

This work was supported by a Grant from the Ministry of Education, Culture, Sports, Science and Technology in Japan awarded to T. Yamasoba. We thank Dr. Y. Kikkawa for valuable advice, Dr. Y. Noguchi of Tokyo Medical and Dental University for DPOAE measurement, and Mr. Y. Mori and Ms. A. Tsuyuzaki for technical assistance.

References

[1] J.H. Abraini, M.C. Gardette-Chauffour, E. Martinez, J.C. Rostain, C. Lemaire, Psychophysiological reactions in humans during an open sea dive to 500 m with a hydrogen-helium-oxygen mixture, J. Appl. Physiol. 76 (1994) 1113–1118.
[2] B.M. Buchholz, D.J. Kaczorowski, R. Sugimoto, R. Yang, Y. Wang, T.R. Billiar, K.R. McCurry, A.J. Bauer, A. Nakao, Hydrogen inhalation ameliorates oxidative stress in transplantation induced intestinal graft injury, Am. J. Transplant. 8 (2008) 2015–2024.
[3] J. Cai, Z. Kang, K. Liu, W. Liu, R. Li, J.H. Zhang, X. Luo, X. Sun, Neuroprotective effects of hydrogen saline in neonatal hypoxia-ischemia rat model, Brain Res. 1256 (2009) 129–137.
[4] J. Cai, Z. Kang, W.W. Liu, X. Luo, S. Qiang, J.H. Zhang, S. Ohta, X. Sun, W. Xu, H. Tao, R. Li, Hydrogen therapy reduces apoptosis in neonatal hypoxia-ischemia rat model, Neurosci. Lett. 441 (2008) 167–172.
[5] J.S. Cardinal, J. Zhan, Y. Wang, R. Sugimoto, A. Tsung, K.R. McCurry, T.R. Billiar, A. Nakao, Oral hydrogen water prevents chronic allograft nephropathy in rats, Kidney Int. 77 (2009) 101–109.
[6] H. Chen, Y.P. Sun, Y. Li, W.W. Liu, H.G. Xiang, L.Y. Fan, Q. Sun, X.Y. Xu, J.M. Cai, C.P. Ruan, N. Su, R.L. Yan, X.J. Sun, Q. Wang, Hydrogen-rich saline ameliorates the severity of L-arginine-induced acute pancreatitis in rats, Biochem. Biophys. Res. Commun. 393 (2010) 308–313.
[7] Y. Fu, M. Ito, Y. Fujita, M. Ito, M. Ichihara, A. Masuda, Y. Suzuki, S. Maesawa, Y. Kajita, M. Hirayama, I. Ohsawa, S. Ohta, K. Ohno, Molecular hydrogen is protective against 6-hydroxydopamine-induced nigrostriatal degeneration in a rat model of Parkinson's disease, Neurosci. Lett. 453 (2009) 81–85.
[8] K. Fujita, T. Seike, N. Yutsudo, M. Ohno, H. Yamada, H. Yamaguchi, K. Sakumi, Y. Yamakawa, M.A. Kido, A. Takaki, T. Katafuchi, Y. Tanaka, Y. Nakabeppu, M. Noda, Hydrogen in drinking water reduces dopaminergic neuronal loss in the 1-methyl-4-phenyl-1,2,3,6-tetrahydropyridine mouse model of Parkinson's disease, PLoS One 4 (2009) e7247.
[9] K. Fukuda, S. Asoh, M. Ishikawa, Y. Yamamoto, I. Ohsawa, S. Ohta, Inhalation of hydrogen gas suppresses hepatic injury caused by ischemia/reperfusion through reducing oxidative stress, Biochem. Biophys. Res. Commun. 361 (2007) 670–674.
[10] D.D. Gehr, T. Janssen, C.E. Michaelis, K. Deingruber, K. Lamm, Middle ear and cochlear disorders result in different DPOAE growth behaviour: implications for the differentiation of sound conductive and cochlear hearing loss, Hear. Res. 193 (2004) 9–19.
[11] K. Hayashida, M. Sano, I. Ohsawa, K. Shinmura, K. Tamaki, K. Kimura, J. Endo, T. Katayama, A. Kawamura, S. Kohsaka, S. Makino, S. Ohta, S. Ogawa, K. Fukuda, Inhalation of hydrogen gas reduces infarct size in the rat model of myocardial ischemia-reperfusion injury, Biochem. Biophys. Res. Commun. 373 (2008) 30–35.
[12] D. Henderson, E.C. Bielefeld, K.C. Harris, B.H. Hu, The role of oxidative stress in noise-induced hearing loss, Ear Hear. 27 (2006) 1–19.
[13] R.H. Julicher, L. Sterrenberg, G.R. Haenen, A. Bast, J. Noordhoek, Sex differences in the cellular defense system against free radicals from oxygen or drug metabolites in rat, Arch. Toxicol. 56 (1984) 83–86.
[14] S. Kajiyama, G. Hasegawa, M. Asano, H. Hosoda, M. Fukui, N. Nakamura, J. Kitawaki, S. Imai, K. Nakano, M. Ohta, T. Adachi, H. Obayashi, T. Yoshikawa, Supplementation of hydrogen-rich water improves lipid and glucose metabolism in patients with type 2 diabetes or impaired glucose tolerance, Nutr. Res. 28 (2008) 137–143.
[15] A. Kashio, T. Sakamoto, K. Suzukawa, S. Asoh, S. Ohta, T. Yamasoba, A protein derived from the fusion of TAT peptide and FNK, a Bcl-x(L) derivative, prevents cochlear hair cell death from aminoglycoside ototoxicity in vivo, J. Neurosci. Res. 85 (2007) 1403–1412.
[16] Y.S. Kikkawa, T. Nakagawa, R.T. Horie, J. Ito, Hydrogen protects auditory hair cells from free radicals, Neuroreport 20 (2009) 689–694.
[17] S.G. Kujawa, M.C. Liberman, Adding insult to injury: cochlear nerve degeneration after "temporary" noise-induced hearing loss, J. Neurosci. 29 (2009) 14077–14085.
[18] K. Nagata, N. Nakashima-Kamimura, T. Mikami, I. Ohsawa, S. Ohta, Consumption of molecular hydrogen prevents the stress-induced impairments in hippocampus-dependent learning tasks during chronic physical restraint in mice, Neuropsychopharmacology 34 (2009) 501–508.
[19] N. Nakashima-Kamimura, T. Mori, I. Ohsawa, S. Asoh, S. Ohta, Molecular hydrogen alleviates nephrotoxicity induced by an anti-cancer drug cisplatin without compromising anti-tumor activity in mice, Cancer Chemother. Pharmacol. 64 (2009) 753–761.
[20] Y. Noguchi, K. Kurima, T. Makishima, M.H. de Angelis, H. Fuchs, G. Frolenkov, K. Kitamura, A.J. Griffith, Multiple quantitative trait loci modify cochlear hair cell degeneration in the Beethoven (Tmc1Bth) mouse model of progressive hearing loss DFNA36, Genetics 173 (2006) 2111–2119.
[21] H. Oharazawa, T. Igarashi, T. Yokota, H. Fujii, H. Suzuki, M. Machide, H. Takahashi, S. Ohta, I. Ohsawa, Protection of the retina by rapid diffusion of hydrogen: administration of hydrogen-loaded eye drops in retinal ischemia-reperfusion injury, Invest. Ophthalmol. Vis. Sci. 51 (2010) 487–492.

[22] K.K. Ohlemiller, Recent findings and emerging questions in cochlear noise injury, Hear. Res. 245 (2008) 5–17.
[23] I. Ohsawa, M. Ishikawa, K. Takahashi, M. Watanabe, K. Nishimaki, K. Yamagata, K. Katsura, Y. Katayama, S. Asoh, S. Ohta, Hydrogen acts as a therapeutic antioxidant by selectively reducing cytotoxic oxygen radicals, Nat. Med. 13 (2007) 688–694.
[24] I. Ohsawa, K. Nishimaki, K. Yamagata, M. Ishikawa, S. Ohta, Consumption of hydrogen water prevents atherosclerosis in apolipoprotein E knockout mice, Biochem. Biophys. Res. Commun. 377 (2008) 1195–1198.
[25] Y. Sato, S. Kajiyama, A. Amano, Y. Kondo, T. Sasaki, S. Handa, R. Takahashi, M. Fukui, G. Hasegawa, N. Nakamura, H. Fujinawa, T. Mori, M. Ohta, H. Obayashi, N. Maruyama, A. Ishigami, Hydrogen-rich pure water prevents superoxide formation in brain slices of vitamin C-depleted SMP30/GNL knockout mice, Biochem. Biophys. Res. Commun. 375 (2008) 346–350.
[26] K. Xie, Y. Yu, Y. Pei, L. Hou, S. Chen, L. Xiong, G. Wang, Protective effects of hydrogen gas on murine polymicrobial sepsis via reducing oxidative stress and HMGB1 release, Shock 34 (2010) 90–97.
[27] K. Xie, Y. Yu, Z. Zhang, W. Liu, Y. Pei, L. Xiong, L. Hou, G. Wang, Hydrogen gas improves survival rate and organ damage in zymosan-induced generalized inflammation model, Shock (2010), doi:10.1097/SHK.0b013e3181def9aa.
[28] T. Yamasoba, A. Pourbakht, T. Sakamoto, M. Suzuki, Ebselen prevents noise-induced excitotoxicity and temporary threshold shift, Neurosci. Lett. 380 (2005) 234–238.
[29] X. Zheng, Y. Mao, J. Cai, Y. Li, W. Liu, P. Sun, J.H. Zhang, X. Sun, H. Yuan, Hydrogen-rich saline protects against intestinal ischemia/reperfusion injury in rats, Free Radic. Res. 43 (2009) 478–484.

J Neurosurg 114:414–425, 2011

Mechanical stress-induced reactive gliosis in the auditory nerve and cochlear nucleus

Laboratory investigation

Tetsuji Sekiya, M.D.,[1] Masahiro Matsumoto, M.D.,[1,2] Ken Kojima, M.D.,[1] Kazuya Ono, B.Pharm.,[1] Yayoi S. Kikkawa, M.D.,[1] Shinpei Kada, M.D.,[1] Hideaki Ogita, M.D.,[1] Rie T. Horie, M.D.,[1] Arpad Viola, M.D.,[3] Matthew C. Holley, Ph.D.,[4] and Juichi Ito, M.D.[1]

[1]Department of Otolaryngology, Head and Neck Surgery, Kyoto University Graduate School of Medicine, Kyoto, Japan; [2]Department of Otorhinolaryngology, University of Tübingen, Germany; [3]Department of Neurosurgery, St. John's Hospital, Budapest, Hungary; and [4]Department of Biomedical Science, The University of Sheffield, England

Object. Hearing levels following microsurgical treatment gradually deteriorate in a number of patients treated for vestibular schwannoma (VS), especially in the subacute postoperative stage. The cause of this late-onset deterioration of hearing is not completely understood. The aim of this study was to investigate the possibility that reactive gliosis is a contributory factor.

Methods. Mechanical damage to nerve tissue is a feature of complex surgical procedures. To explore this aspect of VS treatment, the authors compressed rat auditory nerves with 2 different degrees of injury while monitoring the compound action potentials of the auditory nerve and the auditory brainstem responses. In this experimental model, the axons of the auditory nerve were quantitatively and highly selectively damaged in the cerebellopontine angle without permanent compromise of the blood supply to the cochlea. The temporal bones were processed for immunohistochemical analysis at 1 week and at 8 weeks after compression.

Results. Reactive gliosis was induced not only in the auditory nerve but also in the cochlear nucleus following mechanical trauma in which the general shape of the auditory brainstem response was maintained. There was a substantial outgrowth of astrocytic processes from the transitional zone into the peripheral portion of the auditory nerve, leading to an invasion of dense gliotic tissue in the auditory nerve. The elongated astrocytic processes ran in parallel with the residual auditory neurons and entered much further into the cochlea. Confocal images disclosed fragments of neurons scattered in the gliotic tissue. In the cochlear nucleus, hypertrophic astrocytic processes were abundant around the soma of the neurons. The transverse diameter of the auditory nerve at and proximal to the compression site was considerably reduced, indicating atrophy, especially in rats in which the auditory nerve was profoundly compressed.

Conclusions. The authors found for the first time that mechanical stress to the auditory nerve causes substantial reactive gliosis in both the peripheral and central auditory pathways within 1–8 weeks. Progressive reactive gliosis following surgical stress may cause dysfunction in the auditory pathways and may be a primary cause of progressive hearing loss following microsurgical treatment for VS. *(DOI: 10.3171/2010.2.JNS091817)*

Key Words • **auditory nerve** • **auditory brainstem response** • **cochlear nucleus** • **hearing loss** • **reactive gliosis** • **vestibular schwannoma**

A growing body of evidence indicates that a significant number of patients with VS experience progressive hearing loss following microsurgical intervention. A controlled prospective study has not been performed, and the existing reports are characterized by substantial interpatient variation with respect to hearing level, definition of hearing preservation, and length of the follow-up period. However, hearing loss ranges from 15–40%, within mean follow-up periods of 5–9 years.[5,9,18,32,58,59] In one report as many as 56% of patients (14 of 25) had experienced a decline in hearing quality in the surgically treated ear 20 years after surgery, with only 1 patient experiencing a similar loss in the contralateral ear.[47] Although several explanations have been proposed,

Abbreviations used in this paper: ABR = auditory brainstem response; CAP = compound action potential; CPA = cerebellopontine angle; CR = compression-recording; EDTA = ethylenediaminetetraacetic acid; GFAP = glial fibrillary acidic protein; IAA = internal auditory artery; IAC = internal auditory canal; IAM = internal auditory meatus; IPL = interpeak latency; PBS = phosphate-buffered saline; PNS = peripheral nervous system; TSF = tractus spiralis foraminosus; TZ = transitional zone; VS = vestibular schwannoma.

This article contains some figures that are displayed in color online but in black and white in the print edition.

none has been demonstrated experimentally, and the primary cause remains unknown.

There are several potential causes of hearing loss following surgery. During surgery the contents of the IAC and the surrounding structures in the CPA are mechanically manipulated, which may cause axon degeneration and/or constriction of the arterial blood supply to the cochlea along with fibrosis and scarring in the CPA.[20,47] These reported pathological processes are likely to act together with a combinatorial effect.

Reactive gliosis has not been proposed as a cause, but it is often associated with trauma to the CNS, including that caused by ischemia, radiation, genetic disorders, or chemical insult.[6,13,21,38] A considerable number of quiescent astrocytes can resume proliferation, become hypertrophic, and upregulate GFAP.[19,28,39,52,56]

The mechanical effects of surgery are complex but can be broken down in terms of various forces, such as stretching, laceration, and compression.[7] Evaluating the effects of compression is thus clinically relevant. In this report, we demonstrate for the first time that mechanical compression applied to the auditory nerve induces reactive gliosis not only in the auditory nerve but also in the cochlear nucleus. Various aspects of hearing loss that occur after surgical treatment for VS can best be explained in terms of reactive gliosis combined with additional pathophysiological mechanisms described previously. We emphasize the need to investigate pathological changes not only in the axons but also in the astrocytes to thoroughly understand the mechanisms responsible.

Methods

Inducing Auditory Nerve Degeneration by Compression

Animal experiments were conducted in accordance with the Guidelines for Animal Experiments at Kyoto University. In our experimental model, the axons of the auditory nerve were quantitatively compressed in the CPA without permanent compromise of the blood supply to the cochlea. This was achieved by intraoperative monitoring of CAPs from the auditory nerve as reported elsewhere.[30,43] Briefly, male Sprague-Dawley rats weighing 400–450 grams each were anesthetized by an intraperitoneal injection of ketamine (100 mg/ml; Sankyo Co.) and xylazine (9 mg/ml; Bayer). After exposing the trunks of the seventh and eighth cranial nerves through right retromastoid craniectomy, simulating the same procedure in humans, an L-shaped stainless-steel wire was placed on the auditory nerve as the CR electrode to compress the auditory nerve and simultaneously record the CAPs (Fig. 1). The only device that directly touched the auditory nerve throughout the experiment was this CR electrode. In several rats, the auditory nerve was identified in the CPA and the wound was closed without compressing the nerve. In these rats, the ABRs were completely preserved, and the histological analyses revealed normal cochleae, auditory nerves, and brainstems (data not shown).

In the experimental animals, as the CR electrode was advanced, the auditory nerve was gradually compressed between the tip of the electrode and the rostroventral edge of the IAM (Fig. 1). The cochlear portion of the eighth cranial nerve is located posterodorsally at the IAM level, so the cochlear nerve was directly and highly selectively injured by the CR electrode with the vestibular and facial nerves preserved anatomically.[43] First, the CR electrode was advanced at the speed of 1 μm/second (Positions 1, 2, and 3) until the CAP flattened (Position 4), termed the "flat point," and was maintained at the flat point for 1 minute before the electrode was finally advanced to compress the auditory nerve. Rats in which the CAP recovered within 60 seconds after the flat point was reached, while the CR electrode was maintained at the flat point, were included in this study to ensure that the IAA was still functionally intact after the flat point had been reached. The flattening of the CAP was caused by impairment of the blood supply to the cochlea through the IAA. Recovery of the IAA caused the CAP to reappear spontaneously, while the CR electrode was maintained at the flat point. The critical time of cochlear ischemia that allows for complete recovery of the CAP has been reported to be 5 minutes or more.[2,40] In this experimental model, the cessation of blood supply to the cochlea never exceeded 1 minute in either of the advancements of the CR electrode.

In Group A, the CR electrode was advanced 200 μm from the flat point to compress the auditory nerve. Six rats in this group were studied 1 week after compression and another 6 rats were studied 8 weeks after compression.

In Group B, the electrode was advanced 400 μm, thus increasing the compression damage to the nerve. The same numbers of animals were studied at the same time intervals.

In both groups, the speed of CR electrode advancement was 10 μm/second during the second advancement (the compression procedure); 60 seconds after the start of the second advancement, the electrode was withdrawn at 110 μm/second. The temporal bone on the right side was treated and the left side was used as a control.

Recordings of ABRs and CAPs of Auditory Nerve

Auditory brainstem responses were recorded between the base of the earlobe of the operative side (right) and the vertex, with the ground electrode at the base of the forelimb. Click stimuli (100 dB sound pressure level) were presented to the right ear at a rate of 9.5 pulses/second through a tube earphone or a hollow ear bar driven by a 100-μsec rectangular pulse wave fed by a stimulator. Evoked potentials were amplified with a bandpass of 50 Hz to 3 kHz and averaged using a processor (Synax 1100, NEC Medical Systems) with a sampling interval of 20 μsec and 500 data points in each recording. The responses to 100 successive clicks were averaged for ABR recordings and stored in a computer. Alternating clicks were used to stimulate the ABR. During the first and second compression procedures, the CAPs were recorded between the tip of the CR electrode and the vertex, with the ground electrode placed at the base of the forelimb. For CAP recordings, the acoustic nerve potentials evoked by 5 successive clicks were averaged and stored in a computer. This rate led to a continuous CAP recording rate

of 1 potential every 2.4 seconds before the flat point. The click was picked up at the exit from the earphone with a microphone (ACO 4016, ACO Pacific) connected to the earphone and amplified with a microphone amplifier (MA3, Tucker-Davis Technologies). It was subsequently transferred to an oscilloscope (Iwatsu DS-8812, Iwatsu Electric) for fast Fourier transform analysis, revealing that the frequency of the tones included in the click ranged up to approximately 5 kHz. In contrast to absolute values of amplitudes of ABR, IPLs are relatively independent of the intensity of the stimulus.[11] We measured IPL between Waves I and II (I–II IPL) and IPL between Waves II and IV (II–IV IPL) to investigate the state of nerve impulse conduction from the cochlea to the brainstem. For statistical analyses, unpaired t-tests were performed using Microsoft Office Excel 2007.

Immunohistochemical Analysis

To prepare the temporal bones, each rat was placed in a state of deep anesthesia and was perfused transaortically with 4% paraformaldehyde in 0.01 M PBS at pH 7.4. The temporal bones were decalcified with 10% EDTA and HCl solution (pH 7.4) for 2–3 weeks.

After decalcification, the temporal bones were embedded in OCT compound (Sakura Finetechnical) and frozen. Serial 8-μm sections were then cut for immunohistochemical analysis. Midmodiolar sections included 4 good cross-sections of the Rosenthal canal (basal, lower middle, upper middle, and apical) and the widest part of the auditory nerve. These sections were mounted on glass slides, washed in PBS, and dried at room temperature for 30 minutes. They were permeabilized and then blocked with 10% goat serum in PBS-T (PBS containing 0.2% Triton X-100) at room temperature for 30 minutes.

To visualize astrocytes in the auditory nerve and cochlear nucleus, anti-GFAP rabbit polyclonal antibody (× 500; DAKO) was applied to the sections and incubated at 4°C for 12 hours followed by washing in PBS-T 3 times for 5 minutes each. A secondary antibody (Alexa Fluor 488 goat anti–rabbit IgG antibody × 500, Molecular Probes, diluted with 10% goat serum in PBS-T) was applied to the sections at room temperature for 1 hour followed by washing in PBS-T twice for 5 minutes each time.

To visualize neurons, anti–beta III-tubulin mouse monoclonal antibody (× 500; Covance Research Products, Berkeley) was used as the primary antibody and Alexa Fluor 594 goat anti–mouse IgG antibody (× 500, Molecular Probes) as the secondary antibody.

For nuclear staining, the sections were incubated in 4′,6-diamidino-2-phenylindole (DAPI, 2 μg/ml, Molecular Probes) solution at room temperature for 15 minutes. After being rinsed in PBS, the samples were mounted onto glass slides and coverslipped with VECTASHIELD mounting medium (Vector Laboratories). A fluorescence microscope system equipped with appropriate filters (Olympus BX50 and BX-FLA) was used for observation, and samples were photographed with a digital camera (Olympus DP10). Confocal images were obtained with a confocal laser-scanning microscope (TCS-SP2 Leica Microsystems). Images used for the figures were processed with Photoshop (version 6.0, Adobe Systems).

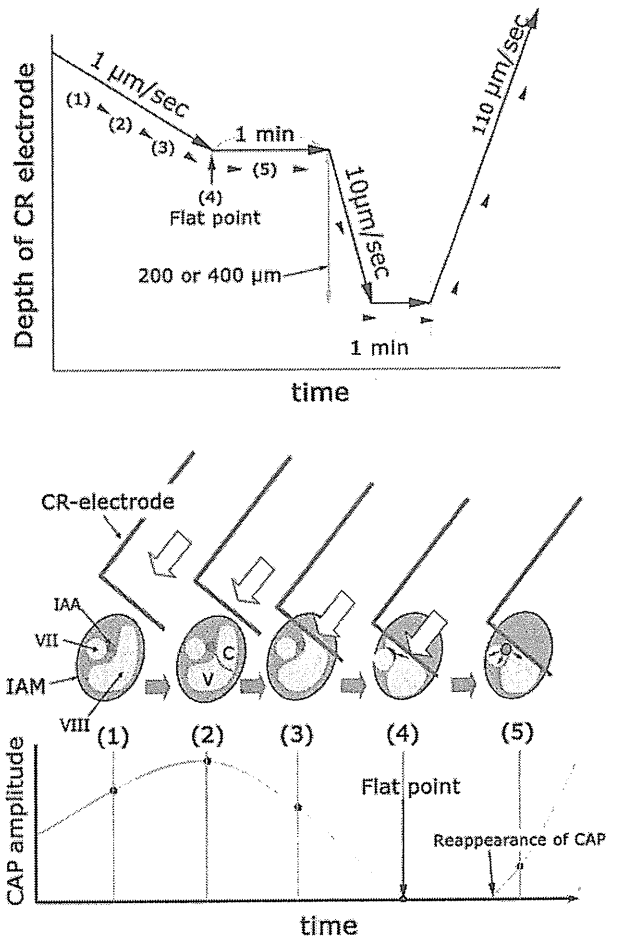

FIG. 1. Mode of advancement of the CR electrode **(upper)** and relationship between electrode depth and amplitude of the auditory nerve CAP during the first advancement of the electrode **(lower)**. **Upper:** First, the CR electrode was advanced at 1 μm/second (CR electrode Positions 1, 2, and 3) until the CAP flattened (Position 4). The CR electrode was maintained at the flat point for 1 minute and then was advanced 200 μm (in Group 1 rats) or 400 μm (in Group 2 rats) at 10 μm/second to compress the auditory nerve; 60 seconds after the start of this advancement, the electrode was withdrawn at 110 μm/second. **Lower:** The IAC contents at the IAM level of the right ear, viewed from the brainstem side toward the cochlea. The CAP amplitude increased as the CR electrode came close to the auditory nerve (Positions 1 and 2) and decreased as the CR electrode continued to be advanced and began to directly compress the auditory nerve due to conduction block of nerve impulses (Position 3). The CAP flattening was caused by impairment of the blood supply to the cochlea through the IAA (Position 4, *small black arrow* indicates collapsed IAA). However, pulsation of the IAA would push the surrounding nerve tissue aside *(small black arrows)*, causing the caliber of the IAA to normalize gradually and the CAP to reappear spontaneously, while the CR electrode was maintained at the flat point (Position 5).

Results

Controls

In a previous paper we demonstrated that a TZ, the interface between the PNS and the CNS portions of the auditory nerve, can be observed even in routine H & E

staining.[44] In our present study the TZ was more clearly observed with anti-GFAP immunostaining because astrocytes are found only in the CNS portion of the auditory nerve (Fig. 2).

At the fundus of the IAC, multiple tiny osseous canals, called the TSF, allow the axons to pass from the Rosenthal canal along the auditory nerve (modiolus) toward the CNS (Figs. 2 and 3).[50]

Throughout the control specimens, the length of the astrocytic processes toward the basal cochlear turn tended to be longer than those toward the middle and apical cochlear turns (Fig. 2 right). It was noted, however, that these astrocytic processes never entered into the TSF in any cochlear turn, even in the basal cochlear turn in controls. With the exception of those in the basal turn, the length of the astrocytic processes never exceeded approximately 75 μm.

Electrophysiological and Morphological Changes After Compression

In rats the CNS portion of the auditory nerve is relatively long, and hence, the TZ is situated within the IAC as in humans (Figs. 2 and 3).[15,53] Because of this anatomical relationship, the compression in the CPA cistern always injured the CNS portion where astrocytes are abundant.

Group A. One week after compression, the general shape of the ABR was preserved but the peak amplitudes were attenuated and the latencies of Waves II, III, and IV were prolonged (Fig. 4). The I–II IPL increased from 0.34 ± 0.03 msec before compression to 0.40 ± 0.03 msec (mean ± SD). The II–IV IPL increased from 0.64 ± 0.03 msec to 0.66 ± 0.04 msec (Fig. 5). The I–II IPL was significantly prolonged after compression ($p < 0.05$) but the II–IV IPL was not. After compression, an unlabeled region was observed just beneath the compression site (Fig. 6). Within this region, GFAP immunoreactivity was lost, indicating the mechanical disruption of the astrocytes. The shape of the TZ was essentially unchanged and the astrocytic outgrowth at the TZ was limited. In the cochlear nucleus we did not observe any change in GFAP staining (data not shown).

Eight weeks after compression the general configuration of the ABR was preserved but the peak amplitude was attenuated and the latencies of Waves II, III, and IV were prolonged (Fig. 7). The latency of the I–II IPL increased from 0.34 ± 0.02 msec to 0.41 ± 0.03 msec ($p < 0.05$) and the II–IV IPL decreased from 0.64 ± 0.01 msec to 0.63 ± 0.03 msec (not significant) (Fig. 5). There was no significant difference in the I–II IPLs between 1 week and 8 weeks after compression. Labeling for GFAP showed that the astrocytic processes elongated enormously from the TZ toward the PNS portion of the auditory nerve (Fig. 8A and B). The length of a substantial number of astrocytic processes was more than 200 μm. The elongated processes ran in parallel with the residual auditory neurons. They entered much further into the TSF in the basal portion of the cochlea compared with the middle cochlear turns (Fig. 8B and C). At the compression site, small, unlabeled areas were observed. Confocal images disclosed a dense meshwork of gliotic tissue at and in the vicinity of the lesion epicenter and fragments of neurons were scattered in this gliotic tissue (Fig. 8D). In the cochlear nucleus, hypertrophic astrocytic processes were abundant around the soma of the neurons (Fig. 8E *single asterisks*) in comparison with the control (Fig. 8F), and in a limited area they formed a meshlike structure of gliotic tissue (Fig. 8E *double asterisks*).

Group B. One week after compression, the ABR was hardly discernible (Fig. 9). Immunohistochemically, a large area unlabeled for GFAP was observed at the compression site (Fig. 10), and it was much larger than that observed in Group A (Fig. 6). The IAC was filled with swollen auditory nerve tissue, a finding not observed in any of the rats in Group A at either time point or in the Group B rats 8 weeks after compression (see below). Astrocytic outgrowth from the TZ was, however, limited (Fig. 10 *large arrowheads*) and in the cochlear nucleus there was no obvious change in GFAP staining (data not shown).

Eight weeks after compression, the peaks of the ABR could not be identified (Fig. 11). The growth of astrocytic processes was much more extensive than in Group A at 8 weeks postcompression (Fig. 12). The length of many processes was more than 300 μm. The astrocytic outgrowth was most evident at the basal portion of the cochlear turn, where the processes elongated and occupied all the orifices of the TSF. Confocal images showed that they ran parallel with the residual auditory neurons within the TSF. In the lesion epicenter, dense gliotic tissue surrounded neural tissue fragments. Similar dense gliotic tissue occupied the cochlear nucleus, where the neurons were tightly surrounded by ramified gliotic tissue. This pathology was only rarely observed in the Group A animals (Fig. 8E). The transverse diameter of the auditory nerve at and proximal to the compression site was reduced considerably, and this finding was more pronounced in this subgroup than in the Group A rats killed at 8 weeks (Figs. 12A and 8A, respectively).

Discussion

In this study we demonstrate for the first time that compression of the auditory nerve induces reactive gliosis not only in the auditory nerve but also in the cochlear nucleus. This can occur even with minimal degradation of the ABR. Thus, reactive gliosis should potentially be regarded as a "third causative factor," in addition to neural and vascular factors, for hearing loss following surgical treatment for VS.

Glial Scar Formation and Degree of Injury

Glial scars are formed in the adult CNS following various insults and constitute a physical and molecular barrier unfavorable to axon survival and regeneration.[6,41,49] In our present study, the gliotic tissue was observed at the lesion epicenter and in the vicinity of the compression site 8 weeks postcompression. Normal tissue architecture was lost, and fragments of auditory neurons were surrounded by reactive astrocytes (Figs. 8D and 12D). Reported ultrastructural findings of degenerating and degenerated

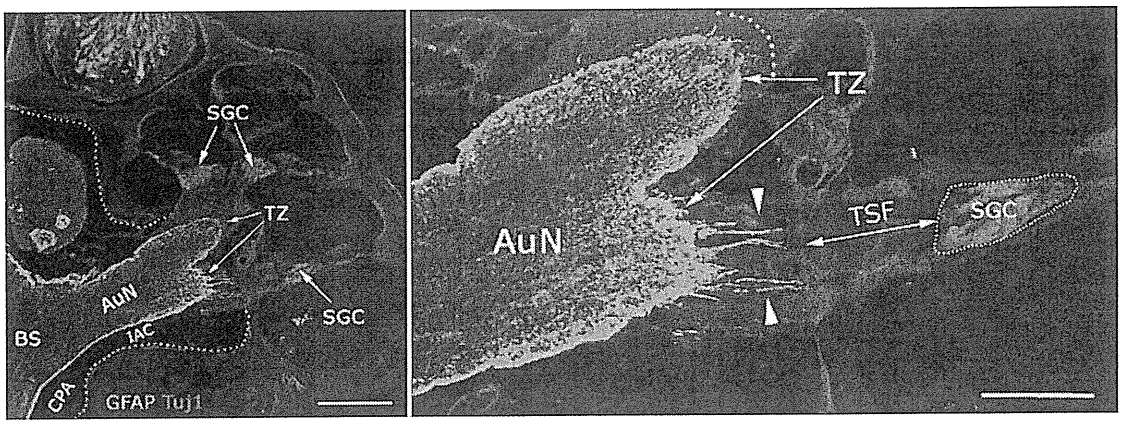

FIG. 2. Photomicrographs showing the TZ of the normal auditory nerve. The interface between the central and peripheral portions of the auditory nerve is clearly observed with anti-GFAP immunostaining *(green)* because of the presence of astrocytes only in the CNS portion of the auditory nerve. Note that the astrocytic processes toward the basal cochlear turn are longer than those toward the other cochlear turns (*arrowheads* in the **right panel**). The astrocytic processes never entered into the TSF in any cochlear turn even in the basal cochlear turn in controls. In this rat, the length of the astrocytic processes from the TZ was less than 75 μm, the longest distance of astrocytic extension in controls in all the cochlear turns except the basal turn (*dotted line* in the **right panel**). The *dotted line* in the **left panel** indicates the border between the intra- and extracranial compartments. Anti-GFAP and anti–beta III-tubulin (clone Tuj1) immunostaining. Bar = 500 μm (left) and 250 μm (right). AuN = auditory nerve; BS = brainstem; SGC = spiral ganglion cell.

axon terminals surrounded and phagocytosed by reactive astrocytes after deafferentation may correspond to our results.[4,10,17,23]

Our results also show that the higher level of compression applied to animals in Group B caused greater degradation of the ABR, increased astrocytic outgrowth from the TZ, higher levels of gliosis in the cochlear nucleus, and larger areas lacking GFAP labeling close to the compression site. In spinal cord injury, the hemorrhagic zone at the lesion epicenter cavitates as a result of necrosis several days after trauma.[22,55] Hemorrhagic foci have been observed previously within the auditory nerve trunk following mechanical trauma.[45] This study shows that they decrease between 1 and 8 weeks after surgery, suggesting invasion by reactive astrocytes. The observed swelling of the auditory nerve within the IAC was much less for low levels of compression and after the longer survival period. Hence, it is likely that swelling occurs only in acute stages of severely compressed auditory nerves, and that it is caused by edema as observed in the optic nerve.[25]

Astrocytic Proliferation and ABR Deterioration

In small experimental animals, Wave I of the ABR is generated from the extracranial (intratemporal bone) portion of the auditory nerve, Wave II reflects synaptic activity in the cochlear nucleus, and the subsequent waves reflect electrical activity in the pons/upper brainstem.[33,46] Because the compression site in our experiments was situated at the IAM, the IPL between Waves I and II was prolonged, but from Wave II through Wave IV the latencies were unaffected.

In our present study, the astrocytic processes elongated conspicuously from the TZ toward the PNS portion of the auditory nerve, ran parallel with the residual auditory neurons, and entered into the TSF, particularly

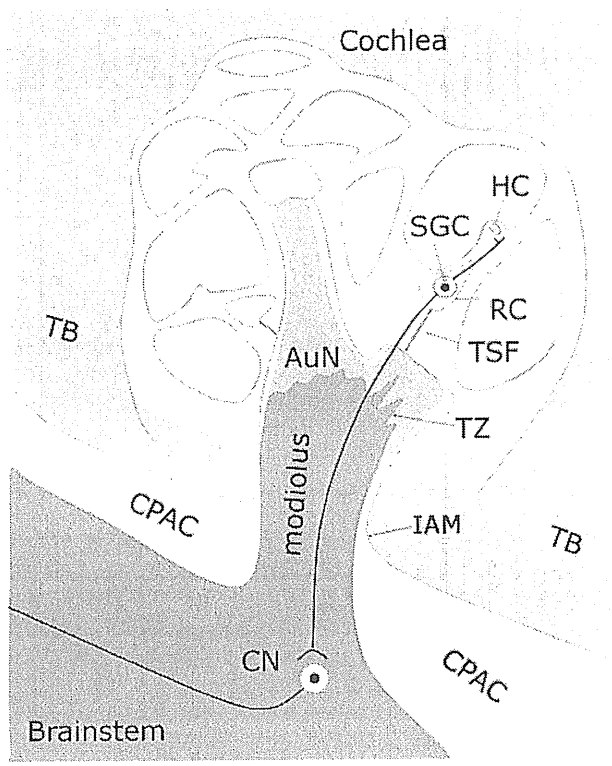

FIG. 3. Schematic illustration showing the anatomical relationships between the auditory nerve and the surrounding structures. The auditory nerve is a bundle of bipolar neurons that form synaptic contacts with the hair cells peripherally and cochlear nucleus cells centrally. The cell bodies of the auditory neurons (spiral ganglion cells) are housed in the Rosenthal canal. The TSF is an osseous canal through which the axons of the auditory nerve pass from the Rosenthal canal to the axis of the auditory nerve (modiolus). CN = cochlear nucleus; CPAC = CPA cistern; HC = hair cell; RC = Rosenthal canal; TB = temporal bone.

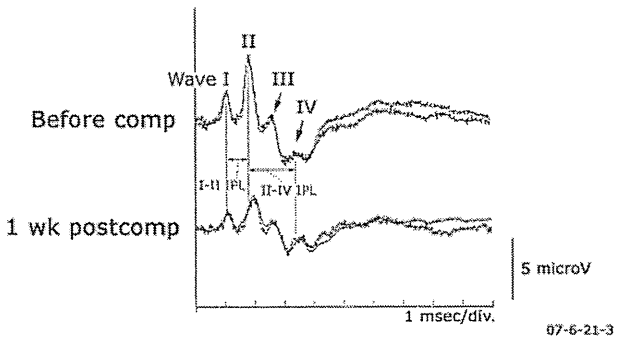

FIG. 4. Auditory brainstem responses in a Group A rat, before and 1 week after compression. The general configuration of the ABR was maintained after compression, but the amplitude of each peak was attenuated and the latencies of Waves II, III, and IV were prolonged. The IPL between Waves I and II (I–II IPL) and that between Waves II and IV (II–IV IPL) before compression are indicated by *doubleheaded horizontal arrows*. Comp = compression.

in the basal region of the cochlea. Massive proliferation of astrocytic processes within the modiolus may physically compress the adjacent nerve fibers, especially within the narrow canals of the TSF. If so, then this could be a cause of hearing loss. Moreover, enhanced glial activity in the region of the cochlear nucleus might have caused both structural and functional changes among synaptic complexes and postsynaptic neurons.[14,16,48] Progressive degeneration of axons has been reported to occur over 8 months and more than 1 year after peripheral insult to the auditory nerve/cochlear nucleus (noise-induced hair cell damage) and spinal cord injury, respectively.[35,57] Thus, the attenuation of Wave II of the ABR may have been caused both by reactive gliosis related to cochlear nucleopathy and by reduction of auditory nerve activity in the cochlear nucleus.

Within Group A, statistically significant differences in the I–II IPLs were not observed between 1 and 8 weeks after compression. However, some auditory nerve degeneration must have developed without being detected in the ABR recordings. Our fast Fourier transform analysis revealed that the click that we used included frequencies up to approximately 5 kHz. The stimulator used was designed for use in humans, and its power spectrum normally stimulates the apical, middle, and upper basal turns of the cochlea; in rats, however, it stimulates only approximately one-quarter of the length of the cochlea.[11,37,60] Thus, the ABRs in our experiments did not cover the potential electrophysiological changes associated with the auditory nerve dysfunction due to the massive outgrowth of astrocytic processes in the lower apical, middle, and basal turns. In one study on rats in which the cochlea was surgically removed, GFAP immunoreactivity increased in the cochlear nuclei 2 days after the surgery, remained intense for 3–8 days, and then declined by Day 21.[12] In another study, the GFAP reaction occurred on Day 1, increased in intensity at Days 4–21, and then remained elevated until Day 45 in the cochlear nucleus (the longest observation time in the study).[8] Our results suggest that

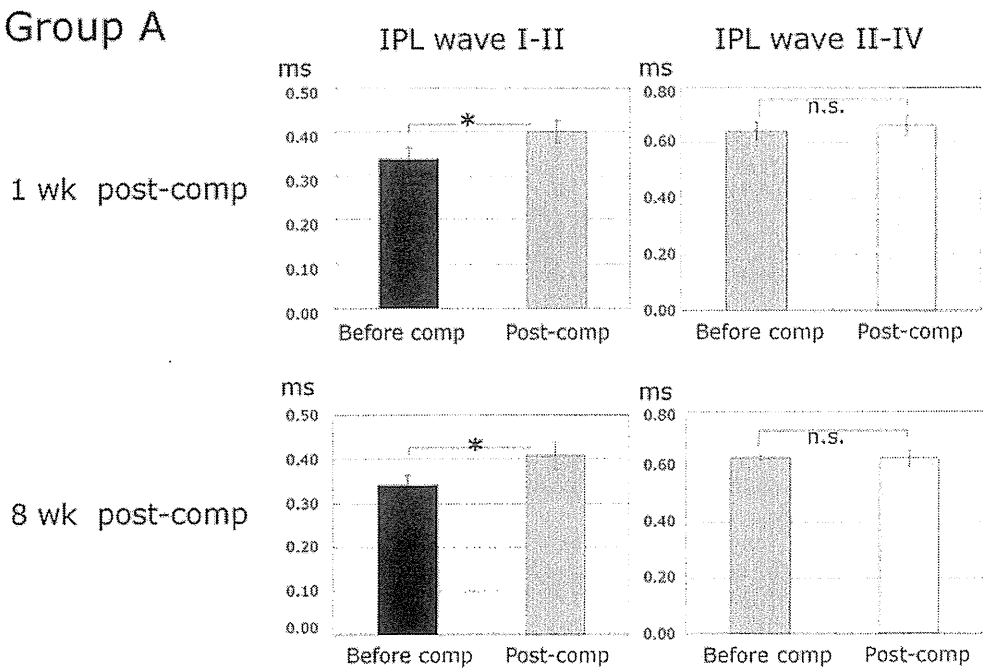

FIG. 5. Bar graphs showing the mean IPLs (± 1 SD) between Waves I and II (I–II IPL) and between Waves II and IV (II–IV IPL), 1 week and 8 weeks after compression in Group A. The I–II IPL was significantly prolonged after compression but the II–IV IPL was not. There was no significant difference between the I–II IPL at 1 week and that at 8 weeks postcompression. ms = msec; n.s. = not significant. * $p < 0.05$.

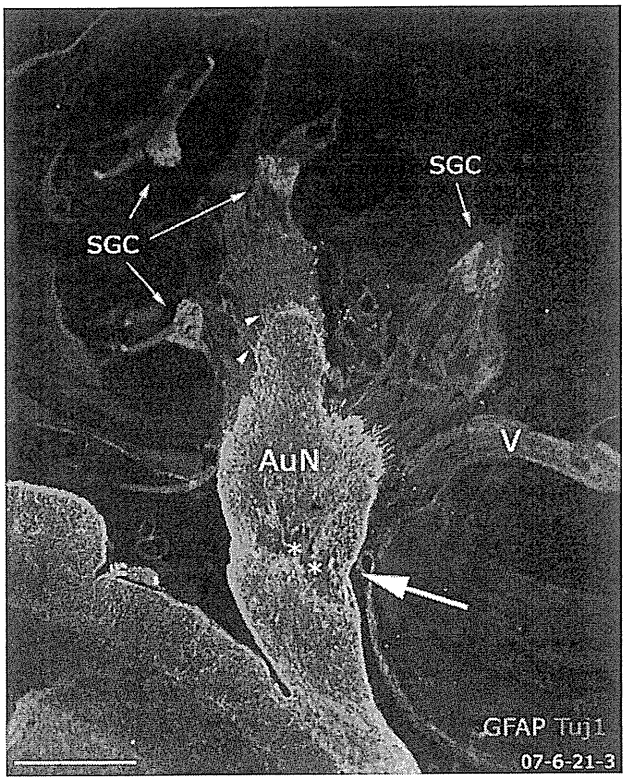

FIG. 6. Photomicrograph showing morphological changes in the auditory nervous system 1 week after compression in Group A (the same rat as in Fig. 4). A GFAP-negative region *(asterisks)* was observed at the compression site *(arrow)*. The shape of the TZ was essentially unchanged *(arrowheads)*. Anti-GFAP and anti–beta III-tubulin (clone Tuj1) immunostaining. Bar = 500 μm. V = vestibular nerve.

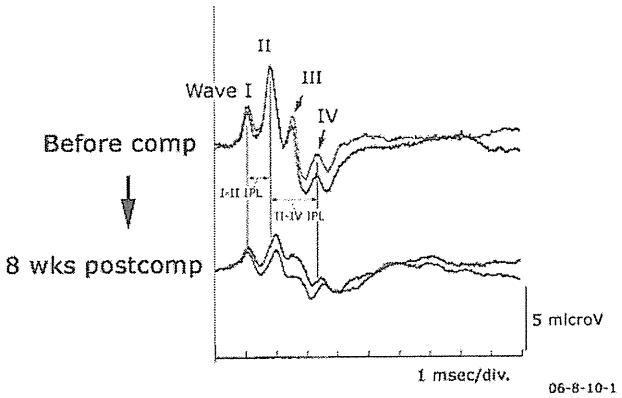

FIG. 7. Auditory brainstem response in a Group A rat, before and 8 weeks after compression. The amplitude was attenuated, but each peak of the ABR was preserved while the latencies of Waves II, III, and IV were prolonged. The I–II IPL and II–IV IPL before compression are indicated by *doubleheaded arrows*.

reactive gliosis continues at least to the 8th week post-compression, and longer-term studies are needed to describe the full consequences of the response.

Clinical Extrapolations

Various clinical observations can be explained by reactive gliosis combined with the previously reported pathophysiological mechanisms. Several reports have demonstrated that the presence of adhesion in the interface between the auditory nerve and the tumor is the most significant negative prognostic factor in hearing preservation surgery, regardless of tumor size.[24,36,51,61] The less adhesion, the less mechanical force needed to separate the auditory nerve from the tumor surface, leading not only to less trauma-induced auditory nerve degeneration but also to less reactive gliosis.

"Cochlear nucleopathy" may "naturally" occur as a VS increases in volume. As the cochlear nuclei are located at the entrance of the fourth ventricle[1] and the shape of the fourth ventricle is inevitably distorted in accordance with tumor growth, the cochlear nuclei cannot escape from the effects of mechanical stress and reactive gliosis. In patients with neurofibromatosis Type 2, the outcome of auditory brainstem implant placement was less favorable in those cases in which the VS compressed and distorted the brainstem than in those in which it did not.[31] In the former, reactive astrocytic proliferation in the cochlear nuclei may have modified synaptic organization leading to less effectiveness of the implant, although larger tumors can be expected to cause more advanced degeneration than smaller ones.

There are some caveats with respect to extrapolation from our results to the situation in human patients. First, the length of the auditory nerve differs markedly between rats and humans. In rats the cisternal portion is approximately 0.5 mm at most (Fig. 2), whereas in humans it is approximately 10–15 mm.[26,34,54] Reactive gliosis may be more severe where the compression site is so much closer to the brainstem.[29,42] Second, in our study the changes to the ABR were created on purpose by traumatizing the "normal" auditory nerve. Under clinical conditions, trauma to the normal auditory nerve may be very rare. In the clinical setting, the ABR configuration in patients with VS is often already distorted before surgical intervention, with the tumor mass causing auditory nerve dysfunction through mechanical compression. This is especially the case with respect to the intracanalicular portion of the auditory nerve. In a study in which the intracanalicular pressure was directly measured in the patients with VS, the pressure within the IAC was significantly elevated, and the authors concluded that pressure from tumor growth in the IAC might be responsible for hearing loss.[3] The morbid auditory nerve in the patients with VS could be significantly more sensitive to the same insult than the normal auditory nerve.[27] Third, we observed ABR decline and remarkable astrocytic proliferation 8 weeks after compression. In contrast, delayed hearing loss has been reported years after surgery in patients who have undergone VS surgery with preserved hearing.[5,9,18,32,58,59] Therefore, our results may be better applied to "subacute" hearing loss in VS surgery. Typically, these patients wake up with hearing after surgery but suffer hearing loss 1–2 months later. However, the time course in gliosis may be different in humans and rats, and it is important to carry

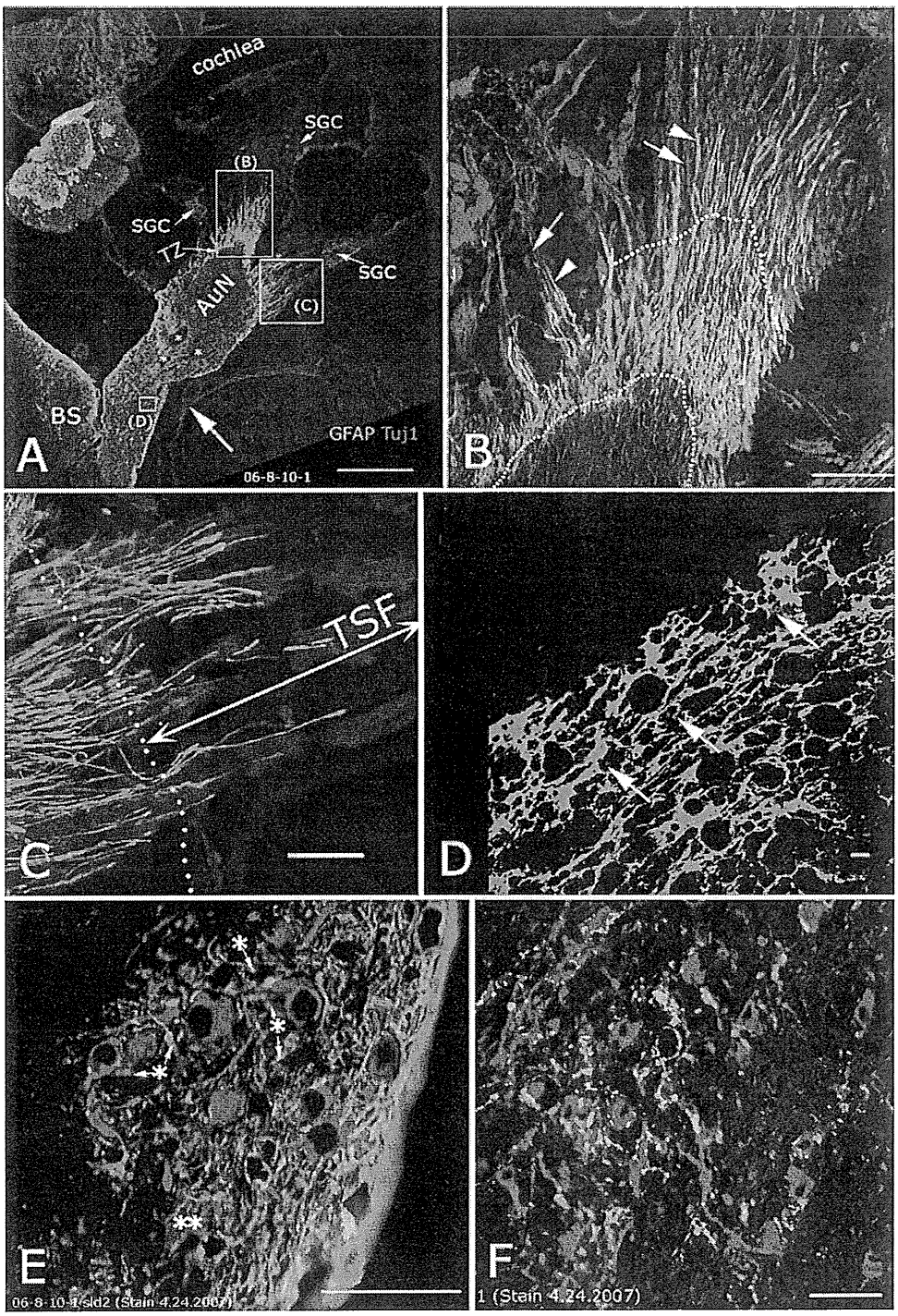

Fig. 8. Morphological changes in the auditory nervous system 8 weeks after compression in Group A (the same rat as in Fig. 7). The astrocytic processes elongated enormously from the TZ toward the periphery (**A and B**). The length of many astrocytic processes was more than 200 μm from the TZ (*dotted lines* in **B**) and they ran parallel with the residual auditory neurons (the *arrowhead* in **B** indicates an astrocytic process and the *arrows*, auditory neurons). The astrocytic processes penetrated the TSF more deeply in the basal portion of the cochlea **(C)** than in the middle portion **(B)**. (Panels **B and C** are enlargements of areas indicated by "(B)" and "(C)" in **panel A**.) At the compression site (*large arrow* in **A**), small, unlabeled areas were observed (*asterisks* in **A**). At and in the vicinity of the lesion epicenter, a dense meshwork of gliotic tissue containing the fragments of neurons (*arrows* in **D**) was observed (the area indicated by "(D)" in **panel A** is enlarged in **panel D**). Hypertrophic astrocytic processes were observed in the cochlear nucleus (*single asterisks* in **E**). Meshlike structure of gliotic tissue was occasionally seen (*double asterisks* in **E**). **F:** Cochlear nucleus region in control. Anti-GFAP and anti–beta III-tubulin (clone Tuj1) immunostaining. Bar = 500 μm (A), 100 μm (B), 100 μm (C), 10 μm (D), 50 μm (E), and 50 μm (F).

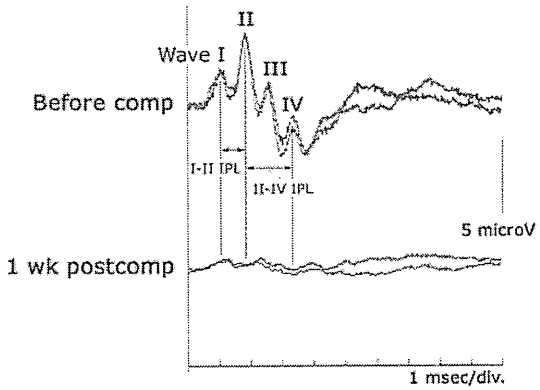

FIG. 9. Auditory brainstem responses in a Group B rat before and 1 week after compression. All the components of ABR were hardly discernible after compression. The I–II IPL and II–IV IPL before compression are indicated by *doubleheaded arrows*.

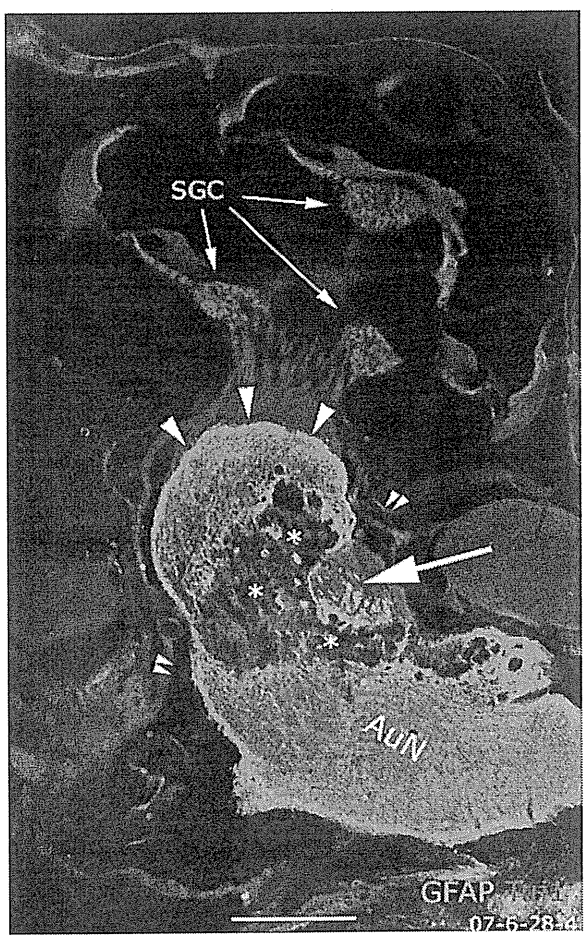

FIG. 10. Morphological changes in the auditory nerve 1 week after compression in a Group B rat (the same animal as in Fig. 9). A large area unlabeled for GFAP *(asterisks)* was observed at the compression site *(arrow)* (compare with Fig. 6). The IAC was filled with swollen auditory nerve tissue. Astrocytic outgrowth from the TZ was limited *(large arrowheads)*. *Small double arrowheads* indicate the IAM. Anti-GFAP and anti–beta III-tubulin (clone Tuj1) immunostaining. Bar = 500 μm. Original magnification × 2.

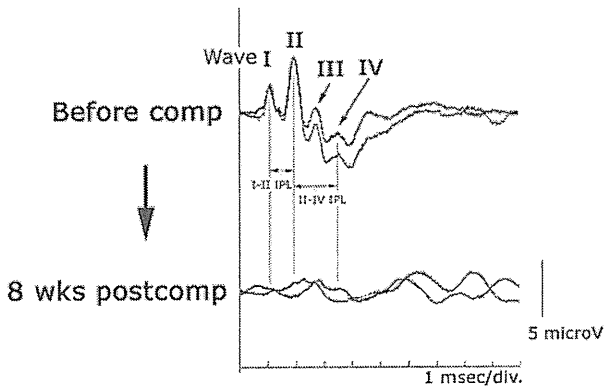

FIG. 11. Auditory brainstem responses in a Group B rat before and 8 weeks after compression. The waveform was not visible after compression. The I–II IPL and II–IV IPL before compression are indicated by *doubleheaded arrows*.

out short- and long-term studies of sequential ABR tracings following surgery in human patients.

Conclusions

We applied compression, a constituent mechanical factor in complex operative procedures, to the auditory nerve of rats while recording ABRs to measure the related hearing loss quantitatively. We found for the first time that a substantial reactive gliosis occurs in both the peripheral and central auditory pathways within 1–8 weeks and is associated with significant degradation of the ABR. This finding warrants further research to test the possibility that in the longer term the gliosis may correlate with and may even cause continued hearing loss. Reactive gliosis may be a primary cause of progressive hearing loss following microsurgical treatment for VS.

Disclosure

The authors report no conflict of interest concerning the materials or methods used in this study or the findings specified in this paper. This study was supported by the Ministry of Education, Culture, Sports, Science and Technology (Japan), the General Insurance Association of Japan, and the Univers Foundation (Japan).

Author contributions to the study and manuscript preparation include the following. Conception and design: T Sekiya. Acquisition of data: T Sekiya, M Matsumoto, K Ono, S Kada, H Ogita, RT Horie, A Viola. Analysis and interpretation of data: T Sekiya, K Ono, MC Holley. Drafting the article: T Sekiya. Critically revising the article: T Sekiya, MC Holley. Reviewed final version of the manuscript and approved it for submission: T Sekiya, M Matsumoto, K Kojima, K Ono, YS Kikkawa, S Kada, H Ogita, RT Horie, A Viola, MC Holley, J Ito. Statistical analysis: T Sekiya. Study supervision: J Ito.

Acknowledgments

The authors appreciate Dr. Agneta Viberg for her useful discussion, and Keiko Nishio, Koichiro Shimomura, Kazumi Sugimoto, and Masashi Higashino for their technical assistance and animal care.

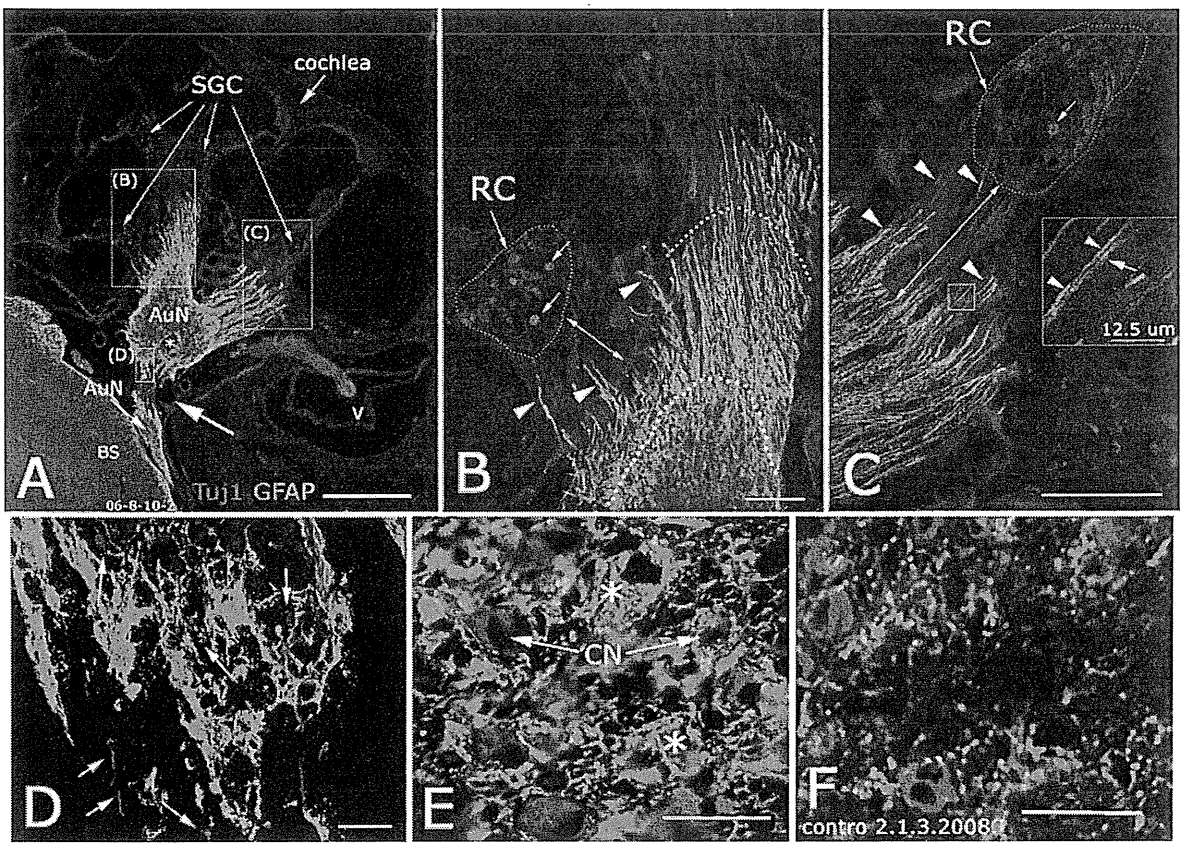

Fig. 12. Morphological changes in the auditory nervous system 8 weeks after compression in a Group B rat (the same animal as in Fig. 11). Extensive astrocytic outgrowth from the TZ was evident (**A–C**). The length of many astrocytic processes was more than 300 μm from the TZ (*dotted lines* in **B**). In the basal turn of the cochlea where the astrocytic outgrowth was greatest, the elongated processes occupied all the orifices of the TSF (*arrowheads* in **C**). The rectangle in C is enlarged in the **inset**; the astrocytic processes (indicated by *arrowheads*) ran parallel with the residual auditory neurons (indicated by *arrow*). In the lesion epicenter, dense plexiform gliotic tissue surrounded neural tissue fragments (*arrows* in **D**). Multiple, small areas unlabeled for GFAP were observed at the compressed site (*asterisk* in A). In the cochlear nucleus, neurons were surrounded by dense gliotic tissue (*asterisks* in **E**; cochlear nucleus region in control, **F**). The transverse diameter of the auditory nerve at and proximal to the compression site was reduced in comparison with that in the Group A rats at 8 weeks postcompression (Fig. 8). The *small arrows* in the Rosenthal canals in **B and C** indicate the residual spiral ganglion cells after compression. Anti-GFAP and anti–beta III-tubulin (clone Tuj1) immunostaining. Bar = 500 μm (A), 100 μm (B), 200 μm (C), 25 μm (D), 25 μm (E), and 25 μm (F).

References

1. Abe H, Rhoton AL Jr: Microsurgical anatomy of the cochlear nuclei. **Neurosurgery 58:**728–739, 2006
2. Asai Y, Umemura K, Nakashima M: Reversibility of compound action potential during the acute phase after transitory local ischemia. **Ann Otol Rhinol Laryngol 105:**472–475, 1996
3. Badie B, Pyle GM, Nguyen PH, Hadar EJ: Elevation of internal auditory canal pressure by vestibular schwannomas. **Otol Neurotol 22:**696–700, 2001
4. Bechmann I, Nitsch R: Astrocytes and microglial cells incorporate degenerating fibers following entorhinal lesion: a light, confocal, and electron microscopical study using a phagocytosis-dependent labeling technique. **Glia 20:**145–154, 1997
5. Betchen SA, Walsh J, Post KD: Long-term hearing preservation after surgery for vestibular schwannoma. **J Neurosurg 102:**6–9, 2005
6. Buffo A, Rite I, Tripathi P, Lepier A, Colak D, Horn AP, et al: Origin and progeny of reactive gliosis: A source of multipotent cells in the injured brain. **Proc Natl Acad Sci U S A 105:**3581–3586, 2008
7. Burnett MG, Zager EL: Pathophysiology of peripheral nerve injury: a brief review. **Neurosurg Focus 16(5):**E1, 2004
8. Campos-Torres A, Touret M, Vidal PP, Barnum S, de Waele C: The differential response of astrocytes within the vestibular and cochlear nuclei following unilateral labyrinthectomy or vestibular afferent activity blockade by transtympanic tetrodotoxin injection in the rat. **Neuroscience 130:**853–865, 2005
9. Chee GH, Nedzelski JM, Rowed D: Acoustic neuroma surgery: the results of long-term hearing preservation. **Otol Neurotol 24:**672–676, 2003
10. Cheng HW, Jiang T, Brown SA, Pasinetti GM, Finch CE, McNeill TH: Response of striatal astrocytes to neuronal deafferentation: an immunocytochemical and ultrastructural study. **Neuroscience 62:**425–439, 1994
11. Chiappa KH: Brain stem auditory evoked potentials: methodology, in Chiappa KH (ed): **Evoked Potentials in Clinical Medicine, ed 2.** New York: Raven Press, 1990, pp 173–221

12. de Waele C, Campos Torres A, Josset P, Vidal PP: Evidence for reactive astrocytes in rat vestibular and cochlear nuclei following unilateral inner ear lesion. **Eur J Neurosci 8:**2006–2018, 1996
13. Eng LF, Ghirnikar RS, Lee YL: Glial fibrillary acidic protein: GFAP-thirty-one years (1969–2000). **Neurochem Res 25:**1439–1451, 2000
14. Eriksson NP, Persson JK, Svensson M, Arvidsson J, Molander C, Aldskogius H: A quantitative analysis of the microglial cell reaction in central primary sensory projection territories following peripheral nerve injury in the adult rat. **Exp Brain Res 96:**19–27, 1993
15. Fraher JP, Delanty FJ: The development of the central-peripheral transitional zone of the rat cochlear nerve. A light microscopic study. **J Anat 155:**109–118, 1987
16. Garrison CJ, Dougherty PM, Kajander KC, Carlton SM: Staining of glial fibrillary acidic protein (GFAP) in lumbar spinal cord increases following a sciatic nerve constriction injury. **Brain Res 565:**1–7, 1991
17. Gentschev T, Sotelo C: Degenerative patterns in the ventral cochlear nucleus of the rat after primary deafferentation. An ultra-structural study. **Brain Res 62:**37–60, 1973
18. Goel A, Sekhar LN, Langheinrich W, Kamerer D, Hirsch B: Late course of preserved hearing and tinnitus after acoustic neurilemoma surgery. **J Neurosurg 77:**685–689, 1992
19. Graeber MB, Kreutzberg GW: Astrocytes increase in glial fibrillary acidic protein during retrograde changes of facial motor neurons. **J Neurocytol 15:**363–373, 1986
20. Johnsson LG, Hawkins JE Jr, Rouse RC: Sensorineural and vascular changes in an ear with acoustic neurinoma. **Am J Otolaryngol 5:**49–59, 1984
21. Julow J, Szeifert GT, Bálint K, Nyáry I, Nemes Z: The role of microglia/macrophage system in the tissue response to I-125 interstitial brachytherapy of cerebral gliomas. **Neurol Res 29:**233–238, 2007
22. Kakulas BA: The applied neuropathology of human spinal cord injury. **Spinal Cord 37:**79–88, 1999
23. Kapadia SE, LaMotte CC: Deafferentation-induced alterations in the rat dorsal horn: I. Comparison of peripheral nerve injury vs. rhizotomy effects on presynaptic, postsynaptic, and glial processes. **J Comp Neurol 266:**183–197, 1987
24. Koos W, Perneczky A: Suboccipital approach to acoustic neurinomas with emphasis on preservation of facial nerve and cochlear nerve function, in Rand RW (ed): **Microneurosurgery, ed 3.** St. Louis: CV Mosby, 1985, pp 335–365
25. Kountakis SE, Maillard AA, Urso R, Stiernberg CM: Endoscopic approach to traumatic visual loss. **Otolaryngol Head Neck Surg 116:**652–655, 1997
26. Lang J Jr, Ohmachi N, Lang J Sr: Anatomical landmarks of the Rhomboid fossa (floor of the 4th ventricle), its length and its width. **Acta Neurochir (Wien) 113:**84–90, 1991
27. Lapsiwala SB, Pyle GM, Kaemmerle AW, Sasse FJ, Badie B: Correlation between auditory function and internal auditory canal pressure in patients with vestibular schwannomas. **J Neurosurg 96:**872–876, 2002
28. Liu L, Rudin M, Kozlova EN: Glial cell proliferation in the spinal cord after dorsal rhizotomy or sciatic nerve transection in the adult rat. **Exp Brain Res 131:**64–73, 2000
29. Liu PH, Yang LH, Wang TY, Wang YJ, Tseng GF: Proximity of lesioning determines response of facial motoneurons to peripheral axotomy. **J Neurotrauma 23:**1857–1873, 2006
30. Matsumoto M, Sekiya T, Kojima K, Ito J: An animal experimental model of auditory neuropathy induced in rats by auditory nerve compression. **Exp Neurol 210:**248–256, 2008
31. Matthies C, Thomas S, Moshrefi M, Lesinski-Schiedat A, Frohne C, Battmer RD, et al: Auditory brainstem implants: current neurosurgical experiences and perspective. **J Laryngol Otol Suppl 27:**32–36, 2000
32. McKenna MJ, Halpin C, Ojemann RG, Nadol JB Jr, Montgomery WW, Levine RA, et al: Long-term hearing results in patients after surgical removal of acoustic tumors with hearing preservation. **Am J Otol 13:**134–136, 1992
33. Møller AR, Burgess J: Neural generators of the brain-stem auditory evoked potentials (BAEPs) in the rhesus monkey. **Electroencephalogr Clin Neurophysiol 65:**361–372, 1986
34. Møller AR, Jannetta P, Bennett M, Møller MB: Intracranially recorded responses from the human auditory nerve: new insights into the origin of brain stem evoked potentials (BSEPs). **Electroencephalogr Clin Neurophysiol 52:**18–27, 1981
35. Morest DK, Kim J, Potashner SJ, Bohne BA: Long-term degeneration in the cochlear nerve and cochlear nucleus of the adult chinchilla following acoustic overstimulation. **Microsc Res Tech 41:**205–216, 1998
36. Moriyama T, Fukushima T, Asaoka K, Roche PH, Barrs DM, McElveen JT Jr: Hearing preservation in acoustic neuroma surgery: importance of adhesion between the cochlear nerve and the tumor. **J Neurosurg 97:**337–340, 2002
37. Müller M: Frequency representation in the rat cochlea. **Hear Res 51:**247–254, 1991
38. Pekny M: Astrocytic intermediate filaments: lessons from GFAP and vimentin knock-out mice. **Prog Brain Res 132:** 23–30, 2001
39. Pekny M, Wilhelmsson U, Bogestål YR, Pekna M: The role of astrocytes and complement system in neural plasticity. **Int Rev Neurobiol 82:**95–111, 2007
40. Perlman HB, Kimura R, Fernandez C: Experiments on temporary obstruction of the internal auditory artery. **Laryngoscope 69:**591–613, 1959
41. Ridet JL, Malhotra SK, Privat A, Gage FH: Reactive astrocytes: cellular and molecular cues to biological function. **Trends Neurosci 20:**570–577, 1997
42. Salvador-Silva M, Vidal-Sanz M, Villegas-Pérez MP: Microglial cells in the retina of Carassius auratus: effects of optic nerve crush. **J Comp Neurol 417:**431–447, 2000
43. Sekiya T, Hatayama T, Shimamura N, Suzuki S: An in vivo quantifiable model of cochlear neuronal degeneration induced by central process injury. **Exp Neurol 161:**490–502, 2000
44. Sekiya T, Kojima K, Matsumoto M, Holley MC, Ito J: Rebuilding lost hearing using cell transplantation. **Neurosurgery 60:**417–433, 2007
45. Sekiya T, Møller AR: Cochlear nerve injuries caused by cerebellopontine angle manipulations. An electrophysiological and morphological study in dogs. **J Neurosurg 67:**244–249, 1987
46. Shaw NA: The auditory evoked potential in the rat—a review. **Prog Neurobiol 31:**19–45, 1988
47. Shelton C, Hitselberger WE, House WF, Brackmann DE: Hearing preservation after acoustic tumor removal: long-term results. **Laryngoscope 100:**115–119, 1990
48. Shortland P, Woolf CJ: Chronic peripheral nerve section results in a rearrangement of the central axonal arborizations of axotomized A beta primary afferent neurons in the rat spinal cord. **J Comp Neurol 330:**65–82, 1993
49. Stensaas LJ, Partlow LM, Burgess PR, Horch KW: Inhibition of regeneration: the ultrastructure of reactive astrocytes and abortive axon terminals in the transition zone of the dorsal root. **Prog Brain Res 71:**457–468, 1987
50. Stjernholm C, Muren C: Dimensions of the cochlear nerve canal: a radioanatomic investigation. **Acta Otolaryngol 122:** 43–48, 2002
51. Strauss C, Bischoff B, Romstöck J, Rachinger J, Rampp S, Prell J: Hearing preservation in medial vestibular schwannomas. **J Neurosurg 109:**70–76, 2008
52. Sumner BE, Sutherland FI: Quantitative electron microscopy on the injured hypoglossal nucleus in the rat. **J Neurocytol 2:**315–328, 1973
53. Tarlov IM: Structure of the nerve root. II. Differentiation of sensory from motor roots: observations on identification of

function in roots of mixed cranial nerves. **Arch Neurol Psychiatry 37:**1338–1355, 1937
54. Tatagiba M, Matthies C, Samii M: Microendoscopy of the internal auditory canal in vestibular schwannoma surgery. **Neurosurgery 38:**737–740, 1996
55. Tator CH: Review of treatment trials in human spinal cord injury: issues, difficulties, and recommendations. **Neurosurgery 59:**957–987, 2006
56. Tetzlaff W, Graeber MB, Bisby MA, Kreutzberg GW: Increased glial fibrillary acidic protein synthesis in astrocytes during retrograde reaction of the rat facial nucleus. **Glia 1:**90–95, 1988
57. Totoiu MO, Keirstead HS: Spinal cord injury is accompanied by chronic progressive demyelination. **J Comp Neurol 486:**373–383, 2005
58. Tucci DL, Telian SA, Kileny PR, Hoff JT, Kemink JL: Stability of hearing preservation following acoustic neuroma surgery. **Am J Otol 15:**183–188, 1994
59. Umezu H, Aiba T, Tsuchida S, Seki Y: Early and late postoperative hearing preservation in patients with acoustic neuromas. **Neurosurgery 39:**267–272, 1996
60. Viberg A, Canlon B: The guide to plotting a cochleogram. **Hear Res 197:**1–10, 2004
61. Yong RL, Westerberg BD, Dong C, Akagami R: Length of tumor-cochlear nerve contact and hearing outcome after surgery for vestibular schwannoma. **J Neurosurg 108:**105–110, 2008

Manuscript submitted December 6, 2009.
Accepted February 16, 2010.
Please include this information when citing this paper: published online April 2, 2010; DOI: 10.3171/2010.2.JNS091817.
Address correspondence to: Tetsuji Sekiya, M.D., Department of Otolaryngology, Head and Neck Surgery, Kyoto University Graduate School of Medicine, Sakyou-ku, Kyoto, 606-8507 Japan. email: tsekiya@ent.kuhp.kyoto-u.ac.jp.

シリーズ　知っておきたい生理・病態の基礎

8. 聴覚末梢

狩野 章太郎

耳鼻咽喉科・頭頸部外科

第82巻　第9号 別刷

2010年8月20日 発行

医学書院

耳喉頭頸　82(9)：631-635，2010

シリーズ　知っておきたい生理・病態の基礎

8．聴覚末梢

狩野章太郎*

Ⅰ はじめに

蝸牛において有毛細胞の上部では基底板の振動が受容器電位に変換され（mechanoelectrical transduction），内有毛細胞と聴神経をつなぐシナプスでは受容器電位がスパイク列に変換される。Mechanoelectrical transduction は外有毛細胞の増幅機構にも関与している。有毛細胞の上下という狭い領域にこのような精緻な機構が存在し，今までは不明な点が多かったがこの 10 年で画期的な知見が続々と得られている。

Ⅱ 内・外有毛細胞の形態と聴神経の接続

ヒトでは一側の耳で 3 万本の聴神経線維が存在する。求心性線維は蝸牛の有毛細胞と脳幹の蝸牛神経核を接続する。らせん神経節細胞の 5～10% が外有毛細胞に接続し，残りが内有毛細胞に接続する[1]。約 20 本の求心性線維が 1 個の内有毛細胞に，また約 6 本の求心性線維が 1 個の外有毛細胞に接続する。内有毛細胞では不動毛は緩い弧状に並び，外有毛細胞では W 字状に並ぶ（図 1）。

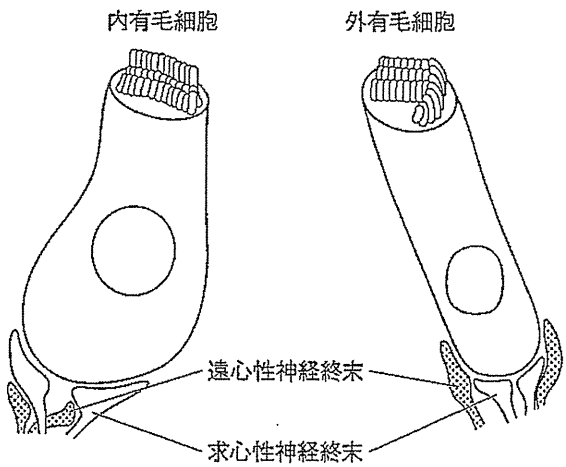

図 1　有毛細胞と聴神経との接続

Ⅲ 有毛細胞の mechanoelectrical ransduction

有毛細胞は不動毛のわずかな屈曲にも敏感に反応し，聴力閾値付近では不動毛の動きは 1 nm 以下と推定される[2]。不動毛はアクチン線維で構成され，不動毛同士は lateral link および ankle link によって連結され束として動く。短いほうの不動毛の先端と長いほうの不動毛をつなぐ tip link があり，不動毛の動きを mechanoelectrical transducer（MET）チャンネルに結びつける[3]（図 2）。Tip link を破壊すると mechanoelectrical transduction は障害され，tip link が再生すると回復した[4]。不動毛の束が長い不動毛の方向に傾くと，MET チャネルが開いてカルシウムイオンが細胞内に流入して脱分極が起こる。短い不動毛方向に傾くと MET チャンネルが完全に閉じて相対的に過分極になる。最近の研究で MET チャンネルは tip link の下端側にだけ存在することが明らかになった[5]。

MET チャンネルが tip link に直接結合してい

＊ かりの　しょうたろう：東京大学医学部耳鼻咽喉科（〒113-0033 東京都文京区本郷 7-3-1）

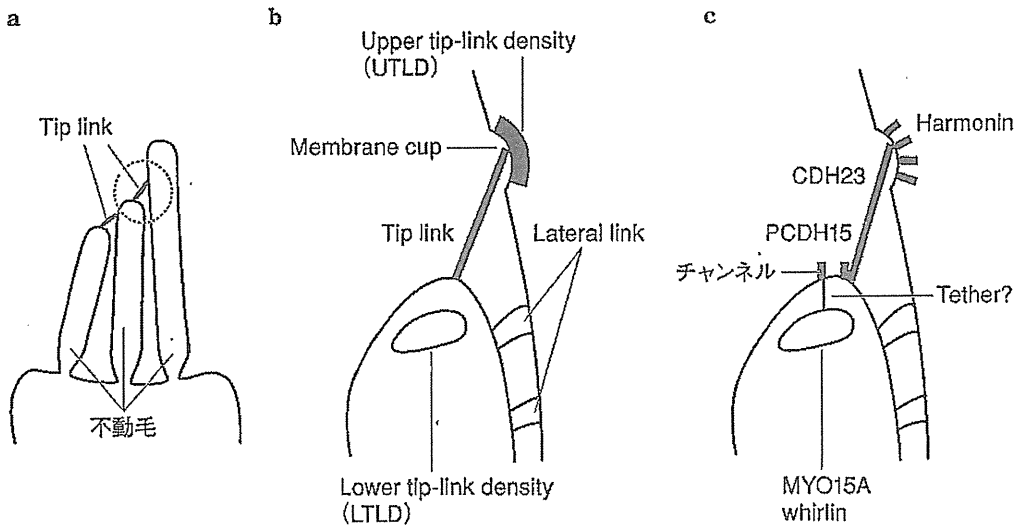

図 2　Hair bundle の構造

a：不動毛と tip link 円内の拡大を b に示す，b：tip link 周辺の構造を示す。
c：b の構造に対応する分子を示す。短いほうの不動毛に mechanoelectrical transducer チャンネルが存在する。

〔文献 6 を一部改変して引用〕

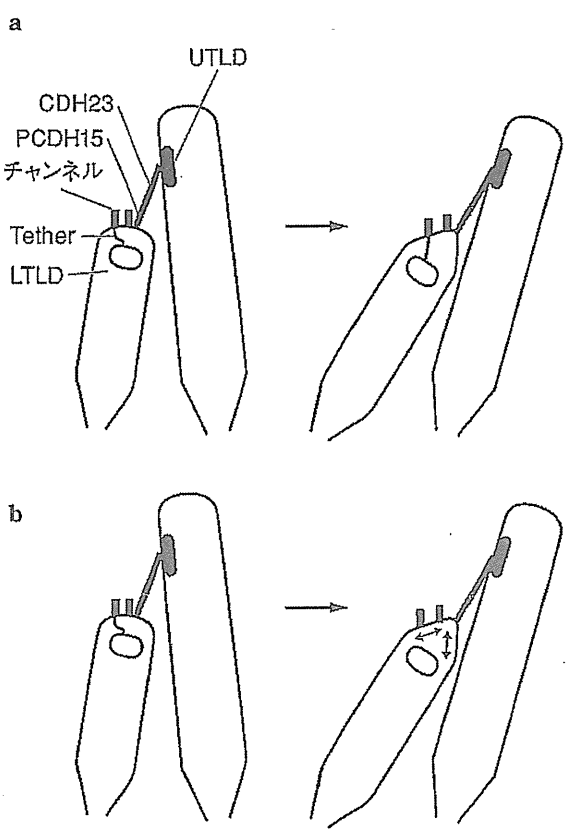

図 3　MET チャンネルが開く機構のモデル

a：MET チャンネルが tip link に直接結合していて不動毛が傾くとチャンネルが開くというモデル
b：細胞膜の張力増加によりチャンネルが開くというモデル

〔文献 6 から一部改変して引用〕

て不動毛が傾くとチャンネルが開くという説と，膜の張力が増大してチャンネルが開くという説がある[6]（図 3）。MET チャンネルは 10 マイクロ秒以内という速度で開くことができ mechnoelectrical transduction のスピードを説明できるが，酵素の働きや拡散ではこのスピードを説明できない[7]。1 本の不動毛当たりの MET チャンネルは 1〜2 個と推定されている[8]。Tip link を構成する分子〔カドヘリン 23（CDH23）やプロトカドヘリン 15（PCDH15）〕が明らかになったのは近年であり[9,10]，MET チャンネルの候補としては transient receptor potential（TRP）チャンネルが挙げられているが，チャンネルの物理的特性が完全には一致せず結論は出ていない[11]。

Ⅳ 有毛細胞の mechanoelectrical transduction とプレスチン

有毛細胞の毛の動きはたかだか 100 nm 程度に過ぎないにもかかわらず，検知できる音圧の範囲（ダイナミックレンジ）は大きい。そのため内有毛細胞が音の情報を聴神経に伝える前の段階で，小さな音圧の刺激は大きな音圧の刺激よりもより強く増幅される必要がある（非線形性）。基底板は音の振動数にあわせて振動するが，その上にのっている外有毛細胞が能動的に動くことで，基底板の

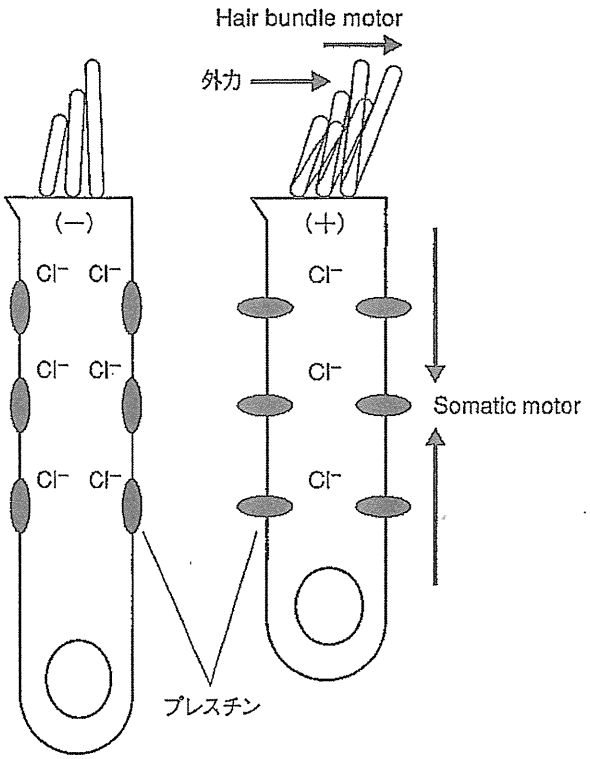

図 4　外有毛細胞が基底板の振動を増幅する機構
静止膜電位（−）においては塩素イオンは膜上の分子プレスチンに結合しているが，不動毛が倒れて脱分極（+）が起こると塩素イオンが外れてプレスチンの立体構造が変わり，外有毛細胞が長軸方向に縮む（somatic motor）。また外力により不動毛が倒れると，不動毛に外力と同じ方向の力が生じて positive feedback が起こる（hair bundle motor）。
〔文献 13 から一部改変して引用〕

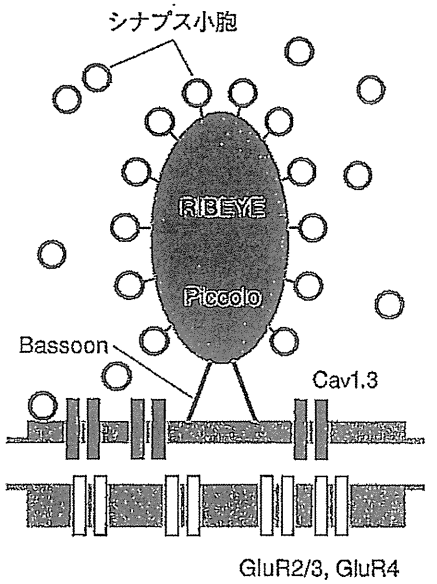

図 5　有毛細胞の active zone に存在するリボンシナプスを構成する分子
〔文献 16 を一部改変して引用〕

振動が増強される。この過程には 2 つの機構が想定されている（図 4）。

1 つは外有毛細胞の外側壁に存在する膜蛋白，プレスチンによるもので，somatic motor と呼ばれる。哺乳類の外有毛細胞は電気刺激によって伸縮することが知られている。前項で述べたように，不動毛が倒れて MET チャンネルが開くと外有毛細胞は脱分極する。静止膜電位のときには塩素イオンがプレスチンに結合しているが，脱分極が起きると塩素イオンが外れてプレスチンの立体構造が変化し，細胞膜上に占める面積が小さくなるために外有毛細胞が縮む[12,13]。

もう 1 つは hair bundle motor と呼ばれる。不動毛が倒れて MET チャンネルが開くとカルシウムイオンが細胞内に流入する。このときラットの場合は不動毛に外力と同じ方向の力が生じて positive feedback が起こることが明らかになっている[14]。MET チャンネルから流入するカルシウムイオンが，脱分極を経てプレスチンによる somatic motor を活性化するほど大きくなくても，hair bundle motor は機能する。Somatic motor は脱分極が必要なので膜の時定数に制限されて高周波の振動に対応できないが，hair bundle motor は高速の MET チャンネルの開閉スピードにのみ制限されるので高周波音の増幅にも対応できると考えられている。

Ⅳ 内有毛細胞と聴神経のシナプス

哺乳類では求心性線維の分岐しない樹状突起の 5〜30 本が 1 つの内有毛細胞とシナプスを形成している[15]。既に all or none の活動電位から始まる通常のシナプスと異なり，リボンシナプスは，アナログ情報である受容器電位を活動電位に変換しなければならない。この過程は，音刺激の特定の位相に同期した聴神経の発火（phase locking）を実現するため，高い時間的精度が求められる。このシナプスは，神経伝達物質を高い時間的精度で連続的に放出するため特化したリボンシナプスと呼ばれ，特別な仕組みがある（図 5）[16]。

有毛細胞の受容器電位の変化により，L 型電位依存性カルシウムチャンネル（Cav1.3）が開いて細胞内カルシウム濃度が増加し，神経伝達物質が

シナプスに放出される。このカルシウムチャンネルはシナプス小胞の多い active zone と呼ばれる狭い領域に集中して存在し，局所的なカルシウム濃度が高くする。1つの active zone に1つのシナプス後端末が接している。さらに1つの active zone に細胞膜につながれたリボンと呼ばれる構造が存在し，その周囲に輪状につながれたシナプス小胞が存在する[17]。リボンの主体は RIBEYE と呼ばれる蛋白質である[18]。Bassoon や Piccolo と呼ばれる分子がリボンを active zone に繋いでいる。Bassoon の遺伝子欠損マウスで放出用のシナプス小胞が減少して，シナプス伝達が不十分になっており[17]，auditory neuropathy との関連が示唆される。

音の周波数をコードするために，このカルシウムチャンネルは 300 マイクロ秒程度の速い時定数をもち，成体では不活化が起きにくくなっており，神経伝達物質を持続的に放出できるので，連続的なシナプス伝達に適している[19,20]。カルシウム濃度の急速な変化に対応するためカルシウム結合蛋白などによる緩衝機能も速い時定数をもつと推定されている[21]。欠損すると難聴の原因となる遺伝子 Otoferlin は，内有毛細胞でカルシウムを検知してシナプス小胞のエキソサイトーシスを引き起こすと考えられているがまだ議論が分かれている[22,23]。有毛細胞内の急激なカルシウムイオン濃度上昇に反応して，マウスの内有毛細胞では最高で1秒間に 3×10^7個程度のシナプス小胞のエキソサイトーシスが起こる[24]。リボンの存在によりシナプス小胞が active zone に集中していることがシナプス伝達の潜時を短くしている[25]。エキソサイトーシスに続いて細胞内に形成されていたシナプス小胞が即座に補充される[26]。受容器電位の生理的な範囲（−50〜−30 mV）では，カルシウムイオンの細胞内流入と求心性線維の活動の関係は線形であり，音圧のコードに歪みが少ないことを意味する[27]。内有毛細胞でグルタミン酸をシナプス小胞に充塡するのは vesicular glutamate transporter3（VGLUT3）であり，この遺伝子が欠損したマウスでは，後述のシナプス後端末の AMPA 受容体が機能していてもシナプス後電流が生じなかった[28]。

シナプス間隙に放出された神経伝達物質は聴神経側のシナプス後端末に存在する AMPA 型グルタミン酸受容体を刺激する[29]。マウスに音響外傷を与えると AMPA 受容体が減少し，その後聴力閾値が改善するとまた増えることが示されており，AMPA 受容体によりシナプス伝達の効率を最適化している可能性が示唆される[30]。聴神経には NMDA 受容体も存在し，サリチル酸が存在すればこれがアラキドン酸の濃度を上げ，NMDA 受容体が刺激されて聴神経の発火頻度を高める[31]。これは NMDA 受容体により聴神経の活動が調整されていることを示唆し，サリチル酸による耳鳴りのモデル[32]に合致する。

文献

1) Spoendlin H：Innervation densities of the cochlea. Acta Otolaryngol 73：235-248, 1972
2) Rhode WS, et al：Model of the displacement between opposing points on the tectorial membrane and reticular lamina. J Acoust Soc Am 42：185-190, 1967
3) Pickles JO, et al：Cross-links between stereocilia in the guinea pig organ of Corti, and their possible relation to sensory transduction. Hear Res 15：103-112, 1984
4) Zhao Y, et al：Regeneration of broken tip links and restoration of mechanical transduction in hair cells. Proc Natl Acad Sci U S A 93：15469-15474, 1996
5) Beurg M, et al：Localization of inner hair cell mechanotransducer channels using high-speed calcium imaging. Nat Neurosci 12：553-558, 2009
6) Gillespie PG, et al：Mechanotransduction by hair cells：models, molecules, and mechanisms. Cell 139：33-44, 2009
7) Corey DP, et al：Kinetics of the receptor current in bullfrog saccular hair cells. J Neurosci 3：962-972, 1983
8) Ricci AJ, et al：Tonotopic variation in the conductance of the hair cell mechanotransducer channel. Neuron 40：983-990, 2003
9) Siemens J, et al：Cadherin 23 is a component of the tip link in hair-cell stereocilia. Nature 428：950-955, 2004
10) Ahmed ZM, et al：The tip-link antigen, a protein associated with the transduction complex of sensory hair cells, is protocadherin-15. J Neurosci 26：7022-7034, 2006
11) Fettiplace R：Defining features of the hair cell mechanoelectrical transducer channel. Pflugers Arch 458：1115-1123, 2009
12) Dallos P：Cochlear amplification, outer hair cells and prestin. Curr Opin Neurobiol 18：370-376, 2008
13) Fettiplace R, et al：The sensory and motor roles of auditory hair cells. Nat Rev Neurosci 7：19-29, 2006
14) Kennedy HJ, et al：Force generation by mammalian hair bundles supports a role in cochlear amplification. Nature 433：880-883, 2005
15) Spoendlin H, et al：The spiral ganglion and the innervation of the human organ of Corti. Acta Otolaryngol 105：403-410, 1988
16) Nouvian R, et al：Structure and function of the hair cell